INTERNATIONAL ATOMIC ENERGY AGENCY
UNITED NATIONS EDUCATIONAL, SCIENTIFIC AND CULTURAL ORGANIZATION
INTERNATIONAL CENTRE FOR THEORETICAL PHYSICS
I.C.T.P., P.O. BOX 586, 34100 TRIESTE, ITALY, CABLE: CENTRATOM TRIESTE

SMR/402 - 35

COLLEGE ON SOIL PHYSICS
9 - 27 October 1989

"Physical Aspects of Growth and Functioning of Plant Roots"

P. RAATS
Institute of Soil Fertility
Haren
The Netherlands

ROLE OF PHYSICISTS IN ROOT ECOLOGY

A. Penetration of roots in soils

B. Uptake and release of water, nutrients, and gases

Scale	Soil	Root	Model
micro	pores	cells	Navier - Stokes
meso	structure	tissue	Richards I
macro	profile	system	Richards II

The physical properties of the soil appropriate for meso- and macro-scale models may differ!

W.R. Gill and R.D. Miller. 1956
A method for study of the influence
of mechanical impedance and aeration
on the growth of seedling roots
Soil Sci. Soc. Amer. Proc. 20: 154-157.

FIG. 2.—Comparison of 50 μ glass beads with a seedling corn root.

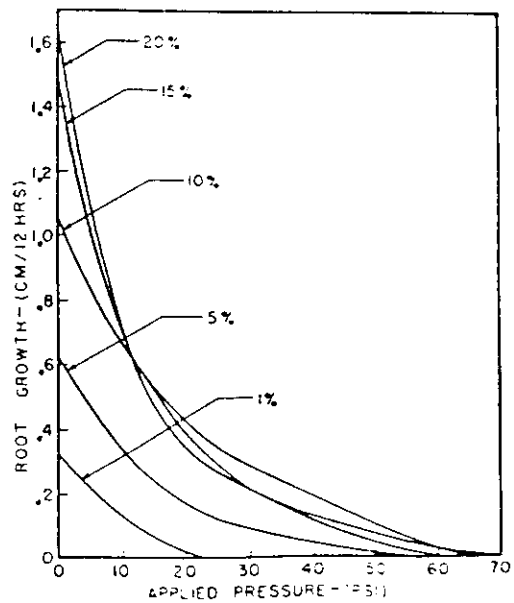

FIG. 3.—Root growth rates as functions of applied diaphragm pressures at various levels of aeration. The numbers on the curves give the percent oxygen values in the root atmosphere.

the kinematics of growing tissues

p.a.c. raats

to be published in: o. diekmann and j.a.j. metz (eds.), dynamics of structured populations. berlin etc., springer, springer lecture notes in biomathematics

Summary

Growth and division of cells are determined on the one hand by genetic properties and on the other hand by the environment in which the growth occurs. Observations related to growth of stems, leaves and roots were reported already in the 18th century. Since 1950 there is also a lot of interest in detailed models for growth of tissues. Most theories proposed thus far are rather special. The purpose of this paper is to formulate a general framework which can accomodate all the earlier work. This helps making the widely spread literature more accessible and removing some of the conceptual confusion.

It is shown that the kinematics of continuous media can be used to describe the growth of tissues. Not only the comparison of tissues at different moments, but also the gradual change of tissues can be dealt with. Cell division is treated on the basis of balance equations for various categories of cells.

Excerpts

The spatial differential balance equation for cells of all sizes is given by

$$\frac{\partial n[t, \underline{x}]}{\partial t} + \nabla.(v[t, \underline{x}]\, n[t, \underline{x}]) = \lambda_n[t, \underline{x}]\, n[t, \underline{x}], \qquad (19)$$

where n is the total number of cells per unit volume, v is the velocity, and λ_n is the number of divisions per cell per unit time. In general integration of this balance equation is difficult. An important exception is 1-dimensional, steady growth for example of a plant root.

Let x be a spatial coordinate coinciding with the axis of a root and attached the mature part of the root. With respect to the x-coordinate, let v be the veloci of any piece of tissue and let w be the velocity of the root tip. Then v - w is th speed of a piece of tissue relative to the root tip. Let y be a spatial coordinate coinciding with the axis of a root with origin at the root tip at all times. Then y is related to t, w, and x by

$y = wt - x.$ (37)

Adding $w\partial n/\partial x$ to both sides of the 1-dimensional form of (19) gives

$$\partial n/\partial t\Big|_x + w\partial n/\partial x = -\partial\{n(v - w)\}/\partial x + \lambda_n n. \quad (38)$$

Introducing (37) into (38) gives

$$\partial n/\partial t\Big|_y = \partial\{n(v - w)\}/\partial y + \lambda_n n. \quad (39)$$

For growth which is *steady in the y-frame*, (39) reduces to

$$\partial\{n(w - v)\}/\partial y = -\lambda_n n, \quad (40)$$

with λ_n and n being merely functions of y. Integration of (40) from y = 0 til y = L gives

$$n(v - w) = \int_0^L \lambda_n \, n \, dy. \quad (41)$$

In (41) the left hand side can be interpreted as the flux of cells relative to the y-frame at y = L and the right hand side can be interpreted as the integral fission rate between y = 0 and y = L (cf. Erickson, 1976, p. 419). If n and (v - w) are measured as functions of y then λ_n can be calculated from equation (40).

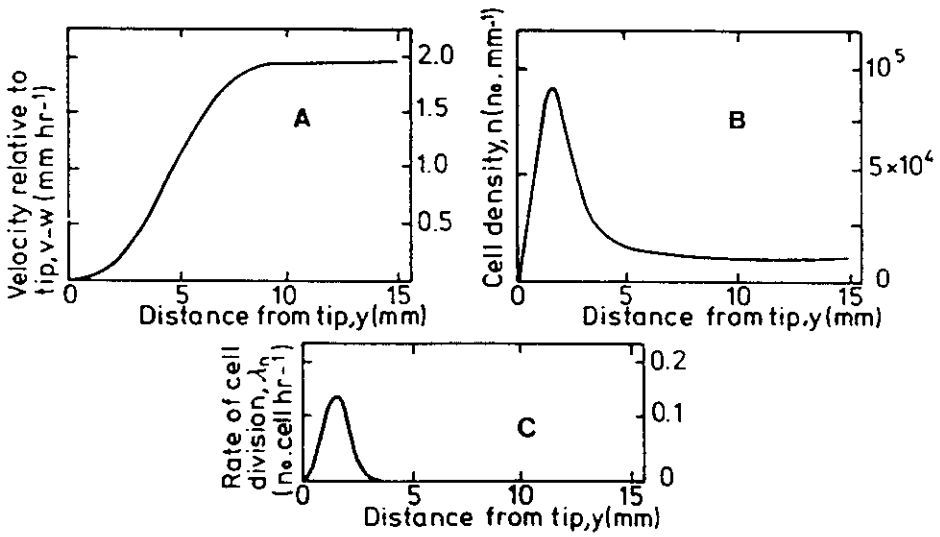

Figure 2. Steady root growth: a. Velocity of pieces of tissue relative to root tip; b. Cell density; c. Rate of cell division; all as functions of distance from root tip (adapted from Erickson, 1976).

Figure 2 shows an example. Note that at large distance from the root tip $\lambda_n \to 0$, and (v - w) and n approach constant values

FROM:

kinematics and dynamics of seedling emergence

p.a.c. raats

in: callebaut, f., d. gabriels and m. de boodt (eds.), assessment of soil surface sealing and crusting. proceedings of the symposium held in ghent, belgium, 1985. ghent, state university; flanders research centre for soil and soil conservation (1986) pp. 252-261

Penetrometers are widely used to assess resistance to penetration by roots and emerging seedlings (Callebout et al., 1985). To interpret penetrometer resistances, theories on the bearing capacity of piles have been a source of inspiration for 20 years. In these theories the soil is assumed behave as a cohesive, frictional (plastic) material near the penetrometer and as a linearly elastic material elsewhere (figure 4).

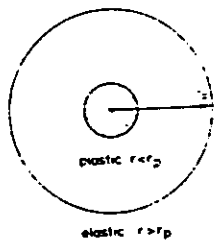

Figure 4. Elastic and plastic zones near a penetrating object.

For a needle penetrometer the deformation will be more or less cylindrical, for a blunt penetrometer more or less spherical. In both the plastic and the elastic zones at each point the forces must satisfy the equilibrium equation:

$$\partial\sigma_r/\partial r = -(N - 1)\ (\sigma_r - \sigma_t)/2, \tag{18}$$

where σ_r is the radial stress and σ_t is the tangential stress, and where N = 2 for cylindrical deformation (needle penetrometer) and N = 3 for spherical deformation (blunt penetrometer).

Distributions of stresses in cylindrical and radial geometries for elastic materials were published already in 1833 by Lamé and Clapeyron. If the boundary between the plastic and elastic zones is located at $r = r_p$ and if the outer boundary of the elastic zone is very far away then σ_r and σ_t are given by

$$\sigma_r = (r_p/r)^N P, \quad \sigma_t = \frac{1}{(N - 1)}\ (r_p/r)^N P, \tag{19}$$

where P is the radial stress at $r = r_p$. Note that with N = 2 (needle penetrometer) $\sigma_r = \sigma_t$, but that with N = 3 (blunt penetrometer) $\sigma_r = 2\sigma_t$.

In the plastic zone the stresses σ_r and σ_t are assumed to satisfy Coulomb's criterion for slip failure in a cohesive, frictional material:

$$\sigma_t = \frac{1 - \sin\phi}{1 + \sin\phi}\,\sigma_r - \frac{2\cos\phi}{1 + \sin\phi}\,c, \tag{20}$$

where c is the cohesion and ϕ is the angle of friction. From (18) and (20) it follows that σ_r and σ_t in the plastic zone are given by:

$$\sigma_r = \{\frac{N}{N-(N-2)\sin\phi}\,(1+\sin\phi)\,(r_p/r)^{2(N-1)\sin\phi}\,(1+\sin\phi)_{-1}\}c\cot\phi \tag{21a}$$

$$\sigma_t = \{\frac{N}{N-(N-2)\sin\phi}\,(1-\sin\phi)\,(r_p/r)^{2(N-1)\sin\phi}\,(1+\sin\phi)_{-1}\}c\cot\phi \tag{21b}$$

Equations (21a) and (21b) reduce to expressions for blunt penetrometers given by Farrell and Greacen (1966) if N = 2 and to expressions for needle penetrometers given by Greacen et al. (1968) if N = 3.

The location of the boundary $r = r_p$ between the elastic and plastic zones is determined by equating the volume of the penetrometer to the change in pore volume. With R known, one can calculate the normal force experienced by the penetrometer. If in addition the angle of friction between penetrometer and soil is known, then one can calculate the penetrometer resistance. For details the reader is referred to the papers by Farrell et al. cited above. Table 1 shows results of calculations for penetration of a Parafield Loam. The required pressure is much larger for spherical than for cylindrical expansion of a cavity. However the resulting penetrometer resistances for the two geometries are similar.

Table 1. Penetration of a Parafield Loam (adapted from Greacen et al. 1968)

Pressure head of soil water (m)	Bulk density of soil g/cm^3	Required pressure for expansion of cavity MPa		Resulting penetrometer resistance MPa			
		Spherical	Cylindrical	Spherical		Cylindrical	
-3	1.5	0.43	0.18	0.66	0.77	0.84	1.05
-3	1.6	0.74	0.29	1.03	1.16	1.34	1.43
-3	1.7	1.19	0.32	1.66	1.94	1.74	2.07
-7	1.5	0.69	0.29	0.97	1.18	1.34	1.50
-7	1.6	1.15	0.45	1.61	1.97	2.13	2.39
-7	1.7	1.99	0.67	2.79	2.76	3.15	3.83

calculated

measured

REFERENCES

Callebaut, F., Gabriels, D., Minjauw, W. and De Boodt, M., 1985. Determination of soil surface strength with a needle type penetrometer. Soil & Tillage Res. 5: 227-245.

Farrell, D.A. and Greacen, E.L., 1966. Resistance to penetration of fine probes in compressible soil. Aust. J. Soil Res. 4: 1-17.

Greacen, E.L., Farrell, D.A. and Cockroft, D., 1968. Soil resistance to metal probes and plant roots. Trans 9th Int. Congr. Soil Sci. Soc. Adelaide, pp. 769-779.

P. de Willigen and M. van Noordwijk
Plant and Soil 77: 215-231, 1984

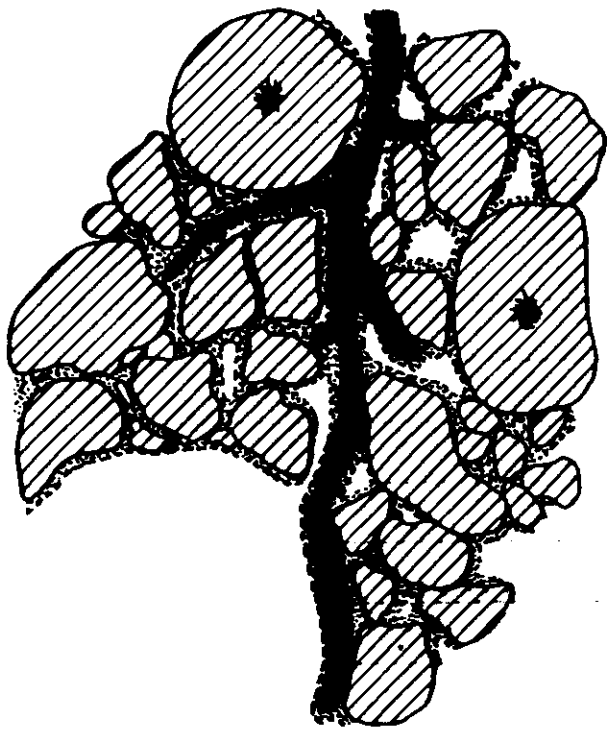

Fig. 1. Schematic representation of a root growing in an aggregated soil (with macropores and micropores) at moderate moisture content. Water films are present around soil aggregates and the root surface. The larger aggregates may contain spots almost permanently anaerobic.

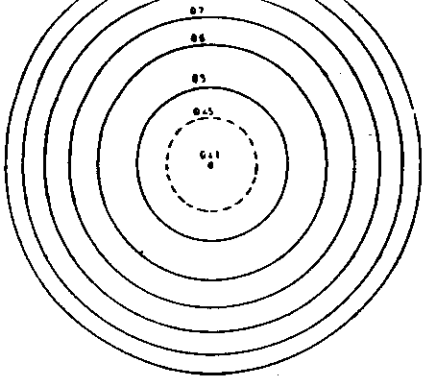

Fig. 6. Isoconcentration lines of oxygen in a root when the entire circumference of the root is exposed to soil air.

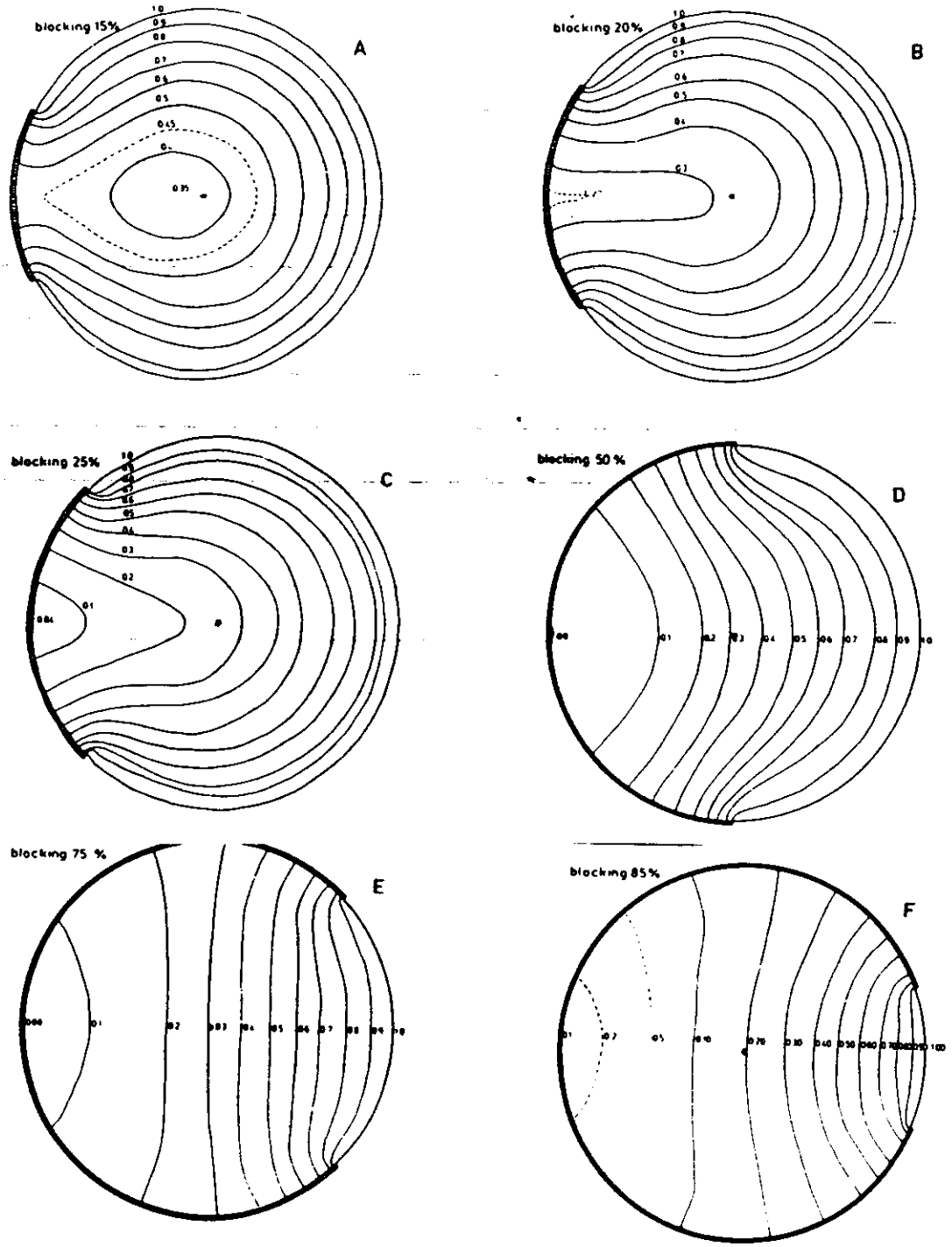

Fig. 7A–F. Isoconcentration lines of oxygen in a root when an increasing part of the root circumference is blocked. A: 15%; B: 20%; C: 25%; D: 50%; E: 75%; F: 85%.

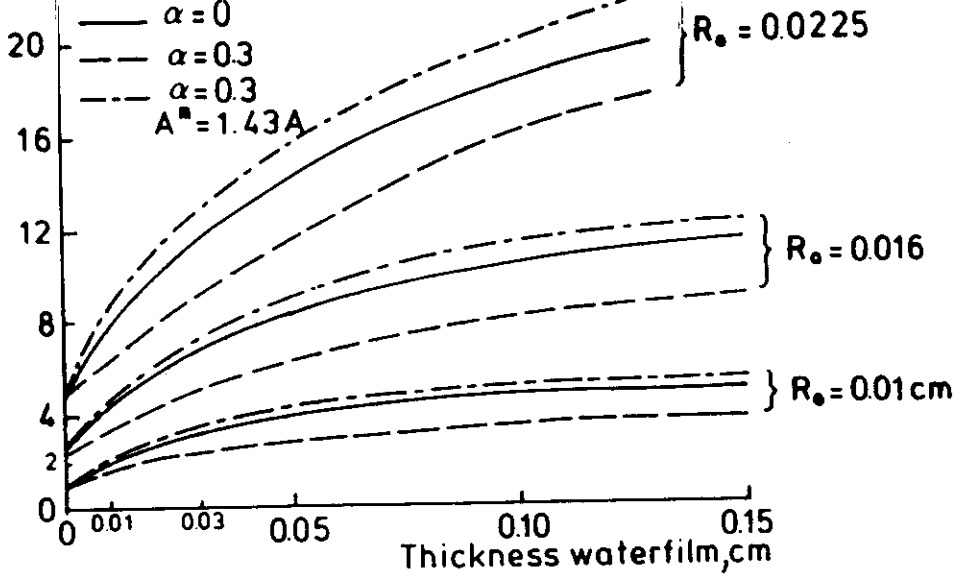

Fig. 1. Oxygen concentration required in soil air for aerobic respiration by all root cells as a function of thickness of the water film a) when respiration is restricted to the root ($\alpha = 0$), b) when the same respiration rate is distributed over root and microbial activity in the water film ($\alpha = 0.3$) and c) when rhizosphere respiration is superimposed on root respiration ($\alpha = 0.03$, $A = 1.43$ A). Results are given for three values of the root radius.

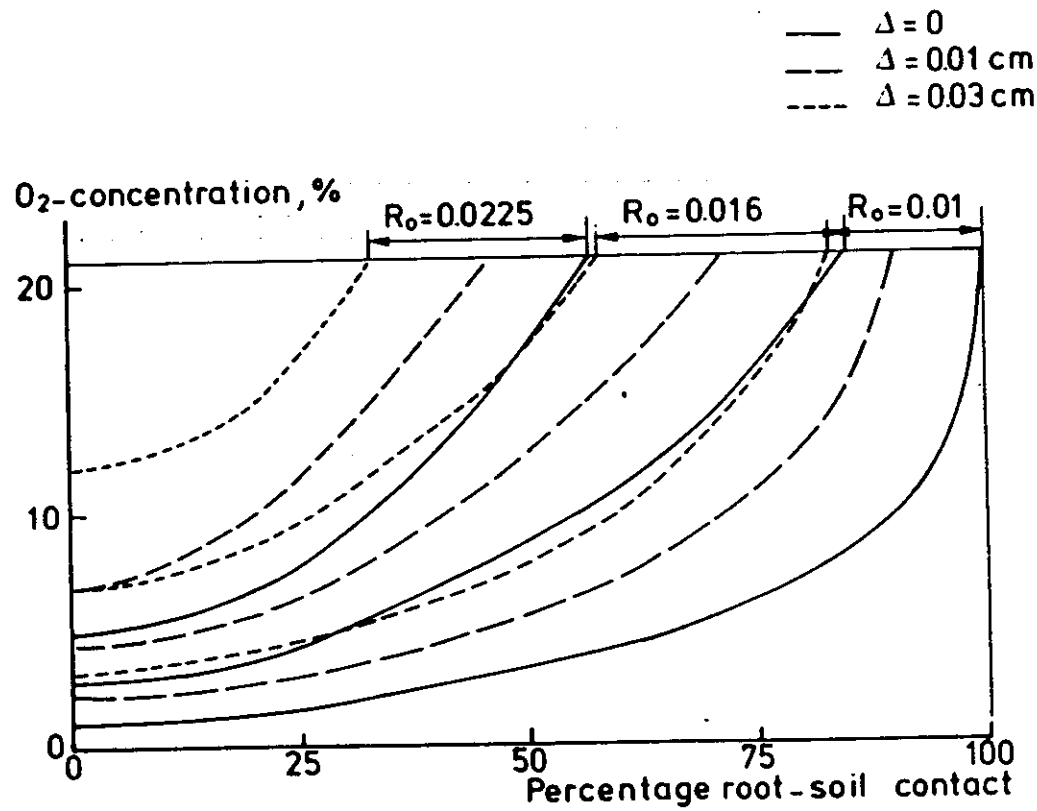

Fig. 2. Oxygen concentration required in soil air for aerobic respiration by all root cells as a function of the percentage of root-soil contact, root radius and thickness of water film (Δ).

UPTAKE OF WATER BY A ROOT

AN INDIVIDUAL

$$\frac{\partial \theta}{\partial t} = \frac{\partial}{\partial r} D \frac{\partial \theta}{\partial r}$$

$t = 0 \qquad r_0 < r < r_1 \qquad \theta = \theta_i$

$t > 0 \qquad r = r_1 \qquad \frac{\partial \theta}{\partial r} = 0$

A. constant rate of uptake

$0 < t < t_{crit} \qquad r = r_0$

$$D \frac{\partial \theta}{\partial r} = \frac{1}{2} \frac{\pi (r_1^2 - r_0^2)}{2 \pi r_1} \frac{E_{pot}}{\delta} = \frac{(r_1^2 - r_0^2)}{4 r_1 \delta} E_{pot}$$

δ depth of root zone

B. falling rate of uptake

$t > t_{crit} \qquad r = r_0 \qquad \theta \rightarrow \theta_{0lim}$

CRITICAL TIME (t_{crit})

Time at which imposed rate of depletion can no longer be sustained.

The critical time is an important characteristic of the entire process.

OTHER PROCESSES INVOLVING CRITICAL TIMES

- evaporation from bare soil - switch from constant rate to falling rate

- rainfall or sprinkler controlled infiltration incipient ponding of water

CHARACTERISTIC LENGTHS ASSOCIATED WITH GEOMETRY OF ROOT SYSTEM

r_0 a) diameter of root
b) internal radius of equivalent hollow cylinder of soil associated with root

r_1 external radius of equivalent hollow cylinder of soil associated with root

TWO CHARACTERISTIC TIMES

1. Characteristic time associated with diffusive transport

$$t_d = \frac{r_1^2}{\bar{D}}$$

2. Characteristic time associated with ratio of supply and demand

$$t_{s/d} = \frac{(\theta_i - \theta_{crit})\,\delta}{E}$$

DIMENSIONLESS VARIABLES

$$\rho = \frac{r}{r_1}$$

$$\tau = \frac{t}{t_d}$$

$$\Delta = \frac{t_{s/d}}{t_d} \frac{\theta_i - \theta}{\theta_i - \theta_{crit}}$$

$$\mathcal{D} = \frac{D}{\bar{D}}$$

UPTAKE OF WATER AT CONSTANT RATE IN TERMS OF DIMENSIONLESS VARIABLES

$$\frac{\partial \Delta}{\partial \tau} = \frac{\partial}{\partial \rho} \mathcal{D} \frac{\partial \Delta}{\partial \rho}$$

$\tau = 0$	$\rho_o < \rho < 1$	$\Delta = 0$
$\tau > 0$	$\rho = 1$	$\frac{\partial \Delta}{\partial \rho} = 0$

A. Constant rate of uptake

$0 < \tau < \tau_{crit}$	$\rho = \rho_o$	$\mathcal{D} \frac{\partial \Delta}{\partial \rho} = \frac{1 - \rho_o^2}{4} \frac{t_d}{t_{d/s}}$

B. falling rate of uptake

$\tau > \tau_{crit}$	$\rho = \rho_o$	$\Delta \rightarrow \Delta_{lim}$

From: PhD thesis of De Willigen and Van Noordwijk (see next page for reference and summary)

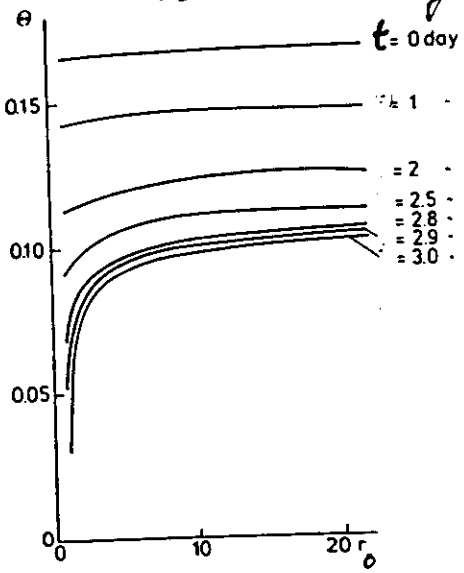

Fig. 9.21 Profile of water content around the root at different times for medium coarse sand, transpiration rate 0.5 cm/day. Root density 1 cm/cm³.

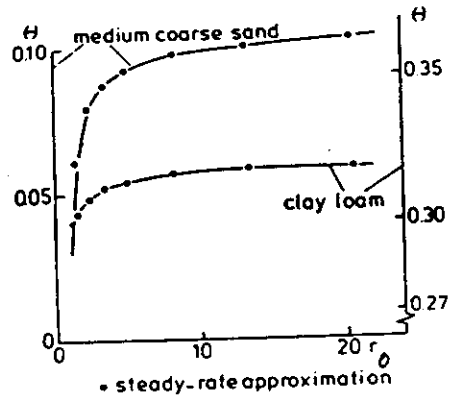

Fig. 9.22 The profile of water content when the matric potential at the root surface equals the limiting value, as calculated with the computer model and via steady rate approximation in the matric flux potential w. Root density 1 cm/cm³, transpiration 0.5 cm/day.

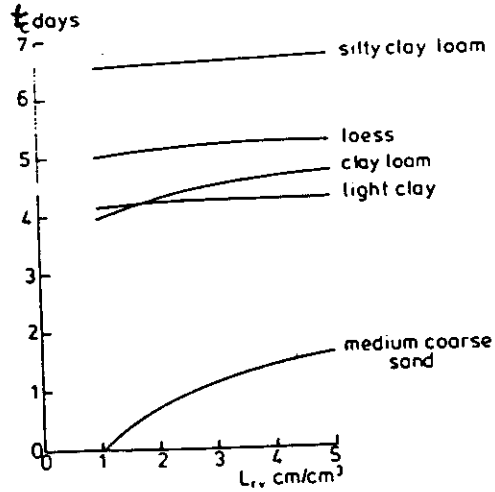

= t_{crit}

Fig. 9.23 Period of unconstrained uptake t_c for water as a function of root density. Transpiration rate 0.5 cm/day.

(root length density

Onderzoek uitgevoerd op het Instituut voor Bodemvruchtbaarheid,
POBox 30003, 9750 RA Haren (Gr.), the Netherlands

Abstract

De Willigen, P and M Van Noordwijk, 1987. Roots, plant production and nutrient use efficiency. PhD thesis Agricultural University Wageningen, the Netherlands, 282 pp, Dutch summary.

The role of roots in obtaining high crop production levels as well as a high nutrient use efficiency is discussed. Mathematical models of diffusion and massflow of solutes towards roots are developed for a constant daily uptake requirement. Analytical solutions are given for simple and more complicated soil-root geometries. Nutrient and water availability in soils as a function of root length density is quantified, for various degrees of soil-root contact and for various root distribution patterns. Aeration requirements of root systems are described for simultaneous oxygen transport outside and inside the root.

Experiments with tomato and cucumber are discussed, which were aimed at determining the minimum root surface area required in an optimal root environment. Experiments on P-uptake by grasses on various soils were performed to test model calculations. Model calculations on the nitrogen balance of a maize crop in the humid tropics suggested practical measures to increase the nitrogen use efficiency.

additional keywords: functional equilibrium, shoot/root ratio, root porosity, Lolium perenne, soil fertility index, sampling depth, synchronization, synlocalization.

Peter de Willigen

Promotor: dr. ir. C.T. de Wit

Co-promotor: dr. ir. P.A.C. Raats.

Meine van Noordwijk

Promotoren: dr. ir. C.T. de Wit,

dr. ir. P.J.C. Kuiper,

Peter de Willigen is eerst verantwoordelijke voor de hoofdstukken 7 tot en met 13
Meine van Noordwijk is eerst verantwoordelijke voor de hoofdstukken 2 tot en met 6, 14 en 16
Hoofdstukken 1 en 15 vallen onder gezamenlijke verantwoordelijkheid.

W.N. Herkelrath, E.E. Miller, and W.R. Gardner, 1977

Water uptake by plants: II. The

root constant model

Soil Sci. Soc. Amer. J. 41: 1039-1043

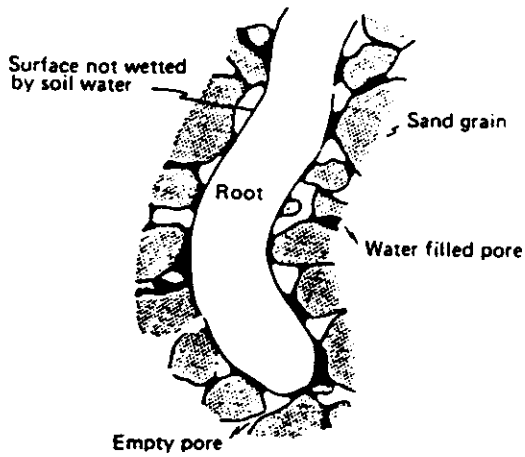

Fig. 3—Poor contact between root and soil.

CONSTANT RATE OF UPTAKE IN PRESENCE OF CONTACT RESISTANCE A LA HERKELRATH, MILLER, GARDNER

$$0 < t < t_{crit} \qquad R = R_0 \qquad D \frac{\partial \theta}{\partial r} = \frac{r_1^2 - r_0^2}{4\, r_1\, \delta} E_{pot}$$

$$- C \frac{\theta_0}{\theta_s} [h[\theta_0] - h_{xylem}]$$

Implicit expression for θ_{0crit}:

$$h[\theta_{0crit}] = h_{xylem\ crit} + \frac{r_1^2 - r_0^2}{4\, r_1\, \delta} \frac{\theta_s}{\theta_{0crit}} \frac{E_{pot}}{C}$$

Expression for uptake of water in SWATRE

DEPENDENCE OF RATE OF UPTAKE UPON THE PRESSURE HEAD

$$S[h] = \alpha[h] * S_{max}$$

$$= \alpha[h] * T/L_r$$

$S[h]$ rate of uptake

$\alpha[h]$ reduction factor

$0 < \alpha < 1$

S_{max} maximum value of S

T potential transpiration

L_r rooting depth

ACTUAL TRANSPIRATION

$$T = \int_{z=0}^{z=L_r} S \, dz$$

REDUCTION FACTOR α AS A FUNCTION OF THE PRESSURE HEAD

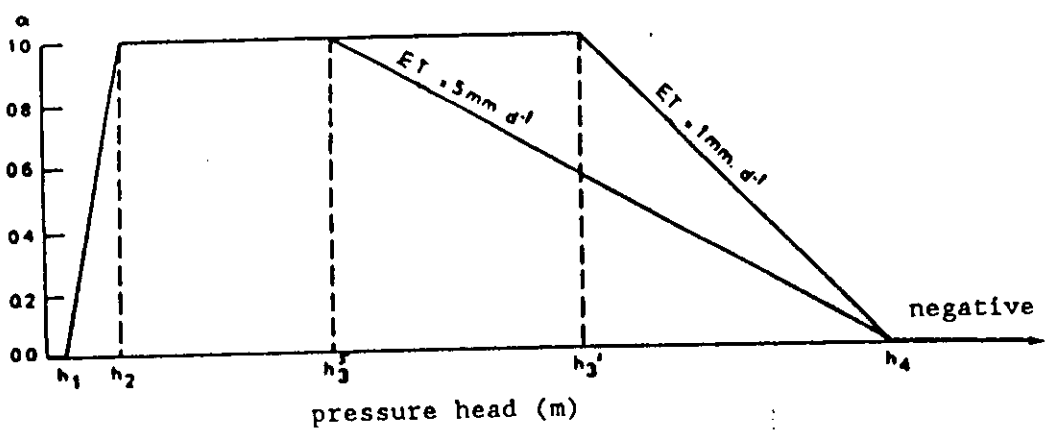

- Example of application of SWATRE

The water balance of the unsaturated zone considered in the context of sustainable agriculture

J.A. de Vos, M.S. Inckel, and P.A.C. Raats

Institute for Soil Fertility, P.O. Box 30003, 9750 RA, Haren, the Netherlands

Sustainable agriculture

The development of sustainable agricultural production systems requires a critical evaluation of the consequences of inputs of fertilizers and organic matter, of soil tillage systems, and the use of biocides. In this context, the Dutch program on soil ecology concentrates on describing the "pools" and "flows" of carbon and nitrogen under field conditions, comparing "conventional" and "integrated" farming systems.

Soil physical conditions

Biological and chemical processes in soil are affected by soil physical conditions, such as soil water content, soil temperature and aeration. These conditions, which vary in time and space, are monitored in the field. The objective is to study the effect of different arable cropping systems on soil ecological factors.

Water balance model

Transport of water in the unsaturated zone is a dominant process in soil. Therefore this process is studied , using the numerical model SWATRE (Feddes,1978). The objectives are to describe the transport of water and solutes for the different cropping systems, to validate the model using field experiments and to use the model for extrapolation purposes.

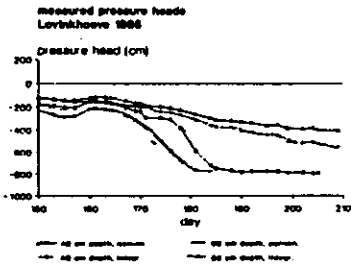

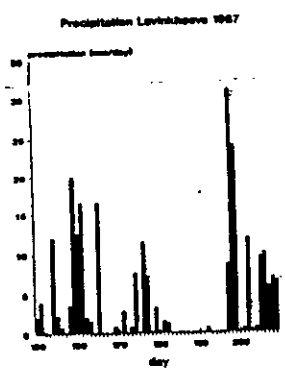

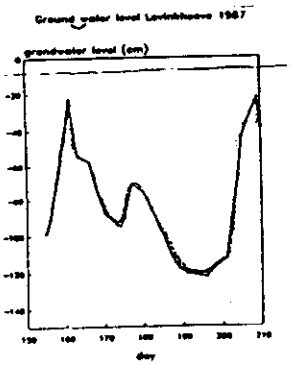

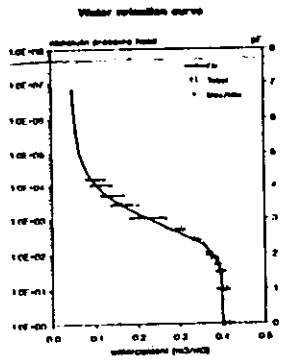

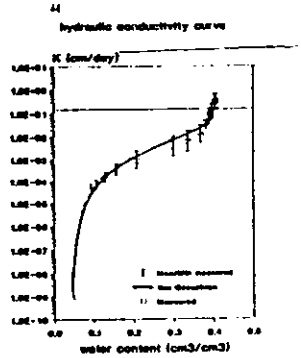

The curves are analytical representations (Van Genuchten, 1978), simultaneously fitted to the measured values.
Plot 12B, topsoil (0 - 30 cm), see Vos (1988).

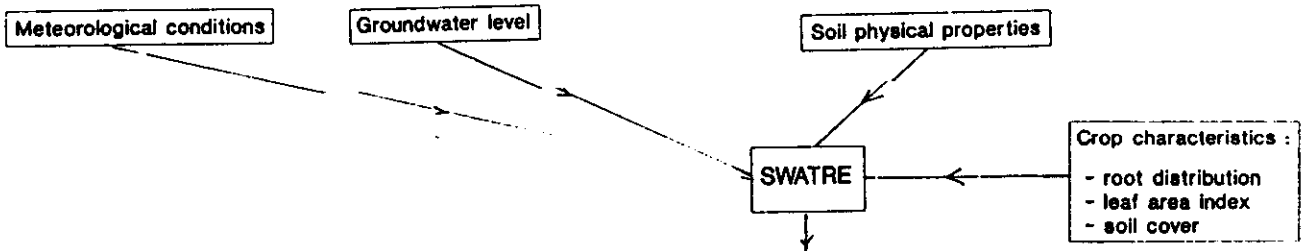

Discussion

The measured pressure heads (1986) showed that different arable cropping systems can result in different soil physical conditions.
The first results of the model SWATRE give a good qualitative representation of the water balance. Better qualitative results can probably be obtained with more accurate input data, such as root distribution, leaf area index and meteorological data. However, sensitivity analysis will be necessary to study the effects of the uncertainties in the input data. Analytical functions for the soil physical properties can be very useful for this purpose.

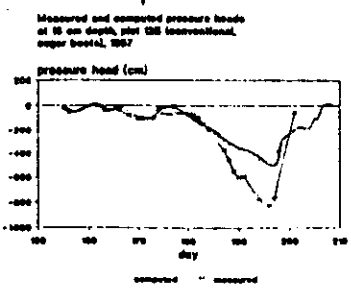

Time-depth-curves of parcels of water and ideal tracers in root-zones

1. Examples of time-depth curves based on a steady state water balance are in:

ABSTRACT

Raats, P.A.C., 1975. Distribution of salts in the root zone. J. Hydrol., 27: 237–248.

Selective uptake of water and convection of salts with the soil water are the main factors governing the distribution of salts in the soil profile. Depth–time trajectories of elements of water are calculated as a function of their initial position, the average soil water content, the uptake distribution, and the rates of irrigation, evaporation, transpiration, and drainage. The mass balance for the salt is reduced to a linear, first-order partial differential equation whose characteristics are the depth–time trajectories of elements of water. Expressions for the increase in salinity along the trajectories are derived. In all specific calculations, it is assumed that the rate of uptake has its maximum at the soil surface and decreases exponentially with depth. As illustrations, depth–time trajectories of elements of water, steady and transient salinity profiles, and the responses of salinity sensors at various depths following a step increase and a step decrease of the leaching fraction are calculated.

2. More recently detailed computer models of the dynamics of water in the root zone have been used to evaluate time-depth curves:

Duynisveld, W. H. M. 1984. Development and application of simulation models for transport of water and solutes in unsaturated soils. Evaluation of the risk of nitrate leaching under arable land. (Ph.D.) Dissertation, Technischen Universität Berlin 204 pp (in German)

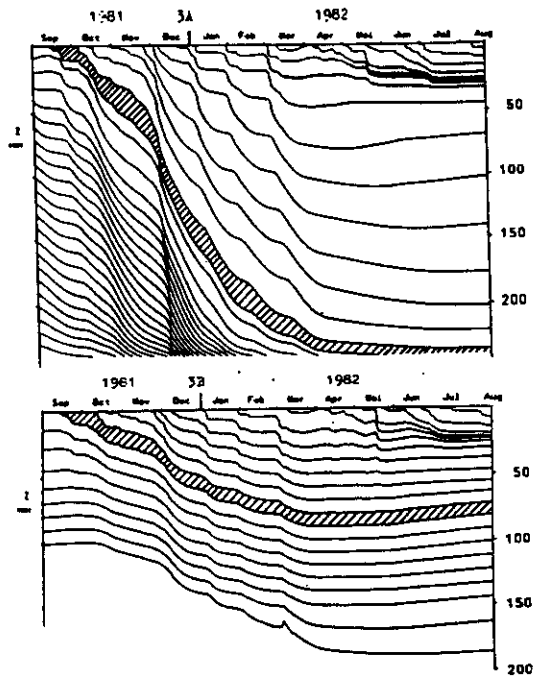

Abb. 3 : Einfluß des Bodens auf Verlagerung und Auswaschung : Zeit-Tiefen-Kurven für zwei grundwasserferne Bodenprofile unter Winterweizen : 3A = Podsol aus feinsandigem Mittelsand, 3B = Parabraunerde aus LöB (bis 1.50 m) über kiesigem Sand

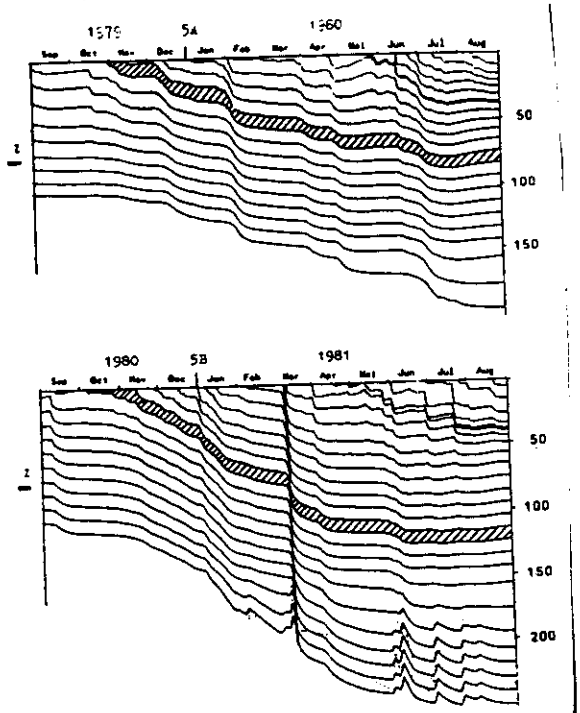

Abb. 5 : Einfluß des Klimas auf Verlagerung und Auswaschung : Zeit-Tiefen-Kurven für eine grundwasserferne LöB-Parabraunerde unter Zuckerrüben für eine niederschlagsarme (=5A) und eine niederschlagsreiche (=5B) Herbst- und Winterperiode

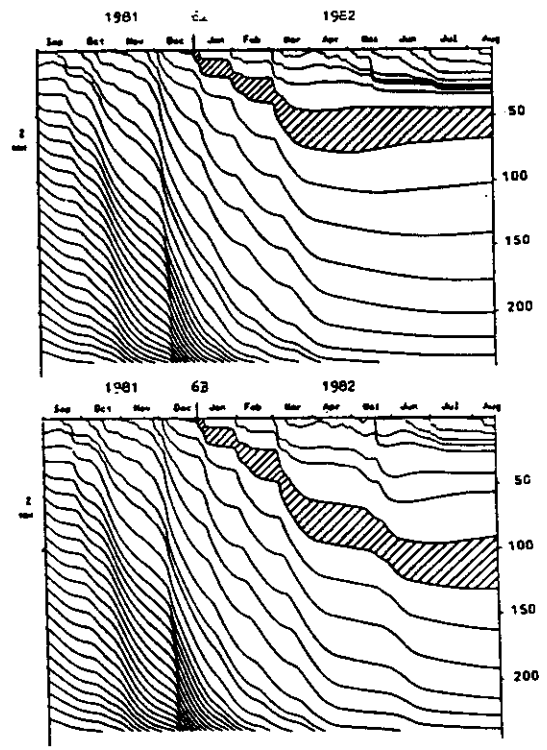

Abb. 6 : Einfluß der Fruchtart auf Verlagerung und Auswaschung : Zeit-Tiefen-Kurven für einen grundwasserfernen Sand-Podsol unter Winterweizen (=6A) und Zuckerrüben (=6B)

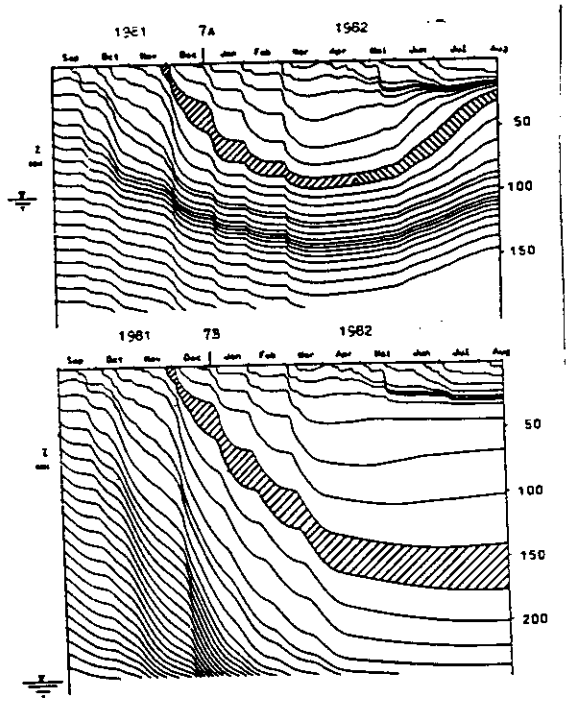

Abb. 7 : Einfluß der Grundwasserflurabstand auf Verlagerung und Auswaschung : Zeit-Tiefen-Kurven für einen grundwassernahen (=7A) und einen grundwasserfernen (=7B) Sand-Podsol unter Winterweizen

water and solutes in the unsaturated zone of the soil. Influence of soil physical properties on water content profiles and time-depth curves. Nota 171. Institute for Soil Fertility, Haren, The Netherlands (in Dutch; paper in English in preparation)

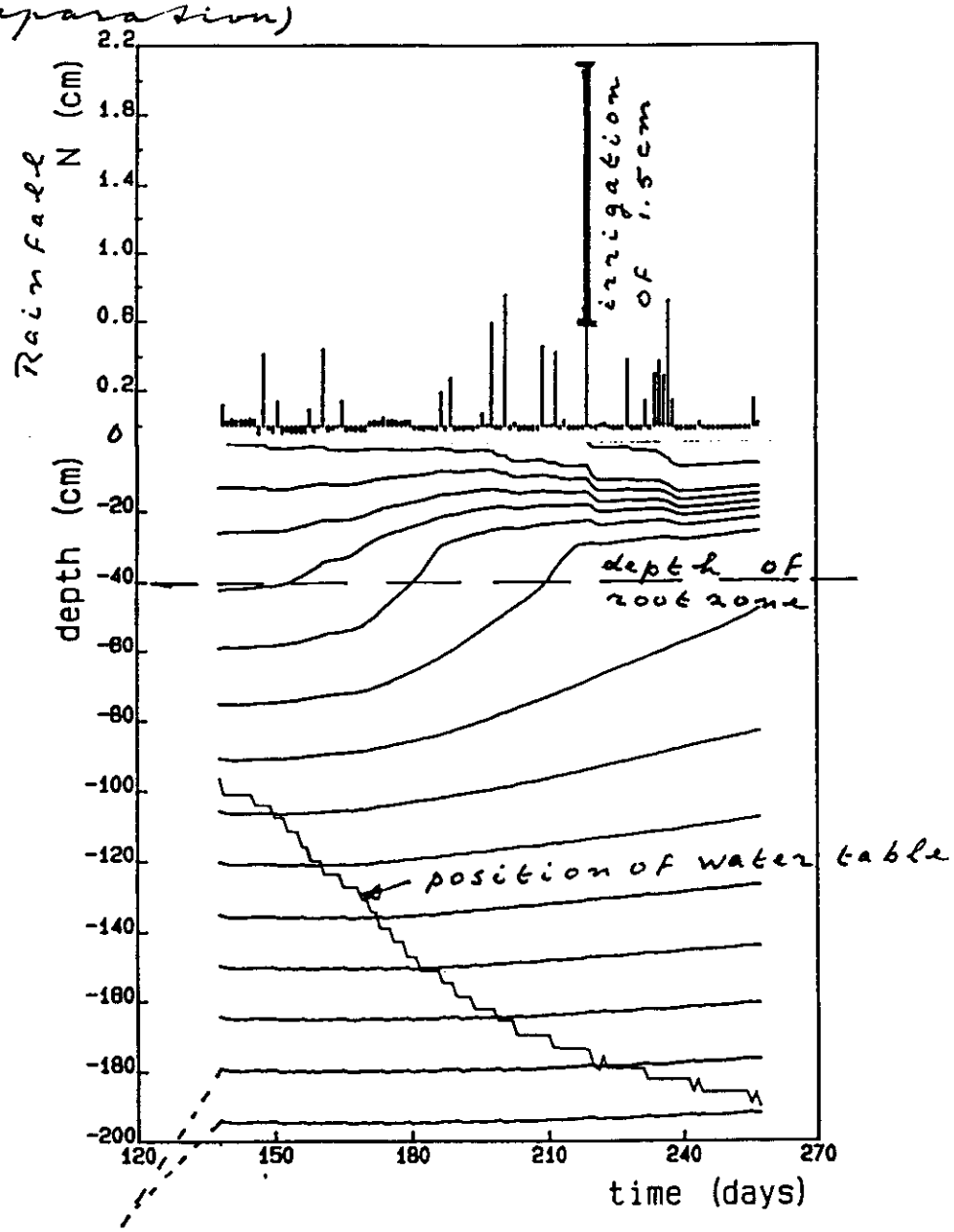

initial spacing of parcels of water is 5cm of water